Available online at www.sciencedirect.com

SCIENCE DIRECT®

Nuclear Instruments and Methods in Physics Research A 560 (2006) 204–210

NUCLEAR INSTRUMENTS & METHODS IN PHYSICS RESEARCH
Section A

www.elsevier.com/locate/nima

# Diffraction field of tightly focused laser beams and its influence to laser accelerator

S.Y. Zhang[a,*], Y.K. Ho[b], Z. Chen[b], Y.J. Xie[b], Z. Yan[b], J.J. Xu[b]

[a]Institute of Condensed Matter Physics, Linyi Normal University, Linyi, Shandong Province 276005, People's Republic of China
[b]Institute of Modern Physics, Fudan University, Shanghai 200433, People's Republic of China

Received 10 May 2005; received in revised form 30 November 2005; accepted 27 December 2005
Available online 30 January 2006

**Abstract**

In this paper, we have studied the dynamic characteristics of relativistic electron injected into stationary intense vacuum laser fields. We found the dynamic trajectories can basically be classified as three categories, namely Inelastic Scattering (IS), Capture and Acceleration Scenario (CAS) and Penetrate into Axial Region and Move (PARM) trajectory. The physical mechanism as to the three kinds of electrons have been examined. In particular, the PARM trajectory which we presented in this paper is different from the CAS and IS trajectory which we had already found in our previous work. We will show the PARM stems from the strong diffraction effect of a tightly focused laser field. In addition, the initial condition for the three kinds of electrons to emerge were detailed investigated. It has been found that there are four factors which chiefly decide the appearance of the three kinds of dynamics trajectories, namely the laser beam width $w_0$ and intensity $a_0$, the electrons incident angle $\theta$ and initial transversal momentum $p_{ti}$. The implication of the PARM electrons to the planned vacuum laser accelerators is illustrated.


*PACS:* 42.50.vk; 42.25.Bs; 42.25.Fx; 52.65.Cc

*Keywords:* Mechanical effects of laser on electrons; Wave propagation; Wave diffraction; Electron trajectory

## 1. Introduction

For more than a decade, we have seen a rapid development in laser intensities [1,2]. Consequently, laser acceleration [3–8] of charged particles has become one of frontier research subjects. In our previous work, we reported a new vacuum laser acceleration scheme, the capture and acceleration scenario (CAS) [8–10].

From our previous papers, the foundation of CAS theory is as follows. For a focused laser beam propagation in vacuum, there exists a subluminous wave phase-velocity region where the phase velocity ($v_\varphi$) is less than the velocity ($c$) of light in vacuum, which emerges just beyond the beam width. There also exists a superluminous wave phase-velocity region near the beam axis where the wave phase velocity ($v_\varphi$) is larger than the velocity ($c$) of light in vacuum. We conclude that there exists an acceleration channel in the field of a focused laser beam propagation in vacuum, which shows similar characteristics to that of a waveguide tube of conventional accelerators: subluminous wave phase-velocity ($v_\varphi < c$) in conjunction with a strong longitudinal electric field component. Consequently relativistic electrons injected into this region can be trapped in the acceleration phase for sufficiently long times, then the electron gains large energy from the laser field.

In order to study CAS as a potential accelerator scheme, we have to examine the dynamic characteristics of relativistic electrons injected into tightly focused intense laser fields. According to our previous numerical simulation result, we found that for wide laser beam width $w_0$ ($kw_0 \geqslant 40$, $k$ is the wave number) and the transverse momentum of the incident electrons ($p_{ti}$) is too small compared with the related ponderomotive potential to penetrate into the beam central region ($p_{ti} < a_0/\sqrt{2}$), where $a_0 = eE_0/(m_e\omega c)$ is a dimensionless parameter measuring

*Corresponding author. Tel.: +86 539 8016639; fax: +86 539 2060903.
*E-mail address:* shaoyizhang@163.com (S.Y. Zhang).

0168-9002/$ - see front matter © 2006 Elsevier B.V. All rights reserved.
doi:10.1016/j.nima.2005.12.246

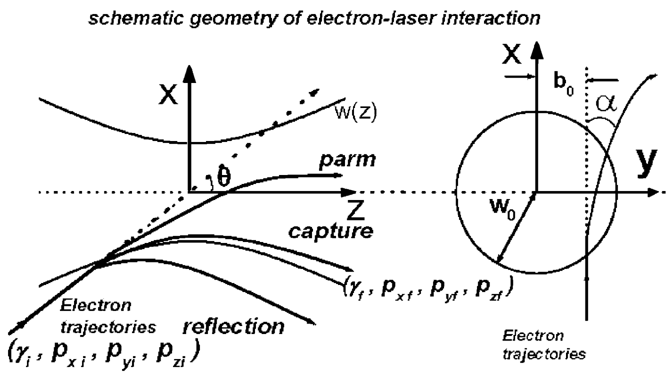


Fig. 1. Schematic geometry of electron being scattered and captured by a laser beam. The laser propagates along the $z$-axis and is polarized in the $x$-direction. The electron comes in from the minus-$x$ side parallel to the $x$–$z$ plane $(\gamma_i, p_{xi}, p_{yi}, p_{zi})$ and $(\gamma_f, p_{xf}, p_{yf}, p_{zf})$ denote the 4-momentum of the electron prior to and after the interaction with the laser beam, respectively. $\gamma$ is the Lorentz factor and $w_0$ is the beam width at the waist. $b_0$ is the impact parameter. $\theta = \tan^{-1}(p_{xi}/p_{zi})$ is the electron incident angle and $\alpha = \tan^{-1}(p_{yf}/p_{xf})$ the deflection angle in the $x$–$y$ plane.

laser intensity, $E_0$ denotes the electric field amplitude of the laser beam at focus, $\omega$ the laser angular frequency, $e$ and $m_e$ the electron charge and mass, respectively, and $c$ the speed of light in vacuum. Under these conditions, the electron trajectories display two kinds, i.e. CAS and inelastic scattering (IS) trajectories (see Fig. 1, the two kinds corresponding to capture and reflection trajectory, respectively). Both groups of electrons reach only the beam surface region. As we extend the study to narrower beam widths ($kw_0 \lesssim 30$), we have found that in addition to the CAS and: IS trajectories, the penetrate into axial region and move (PARM) trajectory emerges (see Fig. 1, the parm trajectory). The conspicuous feature of PARM is the following. Part of the incident relativistic electrons are pushed into the beam central region along their way toward the beam waist, and then move in the beam centrally along trajectories nearly parallel to the beam axis. The main task of this paper is to explore and compare the physics mechanism responsible for the PARM, CAS and IS electrons and examine the conditions under which they will appear. We also discuss the possible implication of PARM electrons to the experimental test of the CAS scheme and to the planned laser accelerators.

## 2. Simulation model

Fig. 1 shows schematically the relevant configuration of the electron–laser interaction, as we had used [8,9]. Throughout this paper, the impact parameter $b_0$ is set to be zero, momentum, length and time are normalized by $m_ec$, $1/k$ and $1/\omega$, respectively. For a Hermite–Gaussian $(0,0)$ mode laser beam polarized in the $x$ direction and propagating along the $z$-axis, the electric component in the polarization direction can be expressed as [11],

$$E_x = E_0\frac{w_0}{w(z)}\exp\left(-\frac{x^2+y^2}{w^2(z)}\right) \times \exp\left[\mathrm{i}\left(kz-\omega t-\varphi(z)-\varphi_0+\frac{k(x^2+y^2)}{2R(z)}\right)\right], \quad (1)$$

where $\varphi_0$ is the laser initial phase,

$$w(z) = w_0\left[1+\left(\frac{2z}{kw_0^2}\right)\right]^{1/2}, \quad (2)$$

$$R(z) = z\left[1+\left(\frac{kw_0^2}{2z}\right)^2\right], \quad (3)$$

$$\varphi(z) = \tan^{-1}\left(\frac{2z}{kw_0^2}\right). \quad (4)$$

Because we study the electron physical processes under the condition of stationary intense laser beam, the disturbance of pulse duration to electron is not considered in this paper. The other electric and magnetic components can be obtained by using following relations:

$$E_Z = (\mathrm{i}/k)(\partial E_x/\partial x), \quad (5)$$

$$\mathbf{B} = -(\mathrm{i}/\omega)\nabla\times\mathbf{E}. \quad (6)$$

The formulae given above are the paraxial approximation expressions. But when $kw_0 < 40$, the paraxial formula may not depict the laser field adequately, high-order corrected [12,13] field model should be used. The transverse electric component in the seventh-order corrected field model can be written as

$$\begin{aligned}E_x = E_0\Big\{&1+s^2(-\rho^2\Theta^2+\mathrm{i}\rho^4\Theta^3-2\Theta^2\xi^2)\\&+s^4\big[2\rho^4\Theta^4-3\mathrm{i}\rho^6\Theta^5-0.5\rho^8\Theta^6\\&+(8\rho^2\Theta^4-2\mathrm{i}\rho^4\Theta^5)\xi^2\big]+s^6\Big[-5\rho^6\Theta^6\\&+9\mathrm{i}\rho^8\Theta^7+2.5\mathrm{i}\rho^{10}\Theta^8-\frac{\mathrm{i}}{6}\rho^{12}\Theta^9\\&-\xi^2(30\rho^4\Theta^6-12\mathrm{i}\rho^6\Theta^7-\rho^8\Theta^8)\Big]\Big\}\psi_0\mathrm{e}^{-\mathrm{i}\varsigma/s^2}, \quad (7)\end{aligned}$$

$$\begin{aligned}E_y = E_0\{&s^2(-2\Theta^2\xi\eta)+s^4[\xi\eta(8\rho^2\Theta^4-2\mathrm{i}\rho^4\Theta^5)]\\&+s^6[-\xi\eta(30\rho^4\Theta^6-12\mathrm{i}\rho^6\Theta^7-\rho^8\Theta^8)]\}\psi_0\mathrm{e}^{-\mathrm{i}\varsigma/s^2}, \quad (8)\end{aligned}$$

$$\begin{aligned}E_z = E_0[&s(-2\Theta\xi)+s^3(6\rho^2\Theta^3-2\mathrm{i}\rho^4\Theta^4)\xi\\&+s^5(-20\rho^4\Theta^5+10\mathrm{i}\rho^6\Theta^6+\rho^8\Theta^7)\xi\\&+s^7(70\rho^6\Theta^7-42\mathrm{i}\rho^8\Theta^8-7\rho^{10}\Theta^9\\&+\mathrm{i}\rho^{12}\Theta^{10}/3)\xi]\Psi_0\mathrm{e}^{-\mathrm{i}\varsigma/s^2}, \quad (9)\end{aligned}$$